IMPROVEMENTS IN THE FRACTURE CLEAVAGE TESTING OF ADHESIVELY-BONDED WOOD

Jerone M. Gagliano
Graduate Research Assistant
Department of Materials Science and Engineering

and

Charles E. Frazier†
Associate Professor
Department of Wood Science and Forest Products
Wood-Based Composites Center
Center for Adhesive and Sealant Science
Virginia Polytechnic Institute and State University
Blacksburg, Virginia 24061-0323

(Received June 2000)

ABSTRACT

Previous researchers have used the contoured dual cantilever beam, DCB, to demonstrate the value of fracture testing for bonded wood. However, use of the contoured specimen is laborious and stringent, preventing the routine application of this powerful test. A simplified method for mode I fracture testing of adhesively-bonded wood is presented here. Two significant improvements are shown: 1) data analysis using a shear corrected compliance method derived from beam theory, and 2) the flat DCB geometry. The shear corrected compliance method is both simple and robust, accounting for variations in wood modulus that often confound traditional shear mode tests. The flat DCB geometry greatly simplifies sample preparation, eliminating difficulties associated with the preparation, calibration, and wood selection that are required with the composite contoured DCB. Real-time crack length measurements required for the flat geometry are routine using digital hardware. The sensitivity and simplification of the method are presented in hopes of promoting the wider adoption of fracture testing for bonded wood.

Keywords: Fracture test, cleavage, wood adhesion.

INTRODUCTION

Several test methods are commonly used to evaluate wood adhesive performance, and all have their various shortcomings. For example, many R&D personnel are familiar with the difficulties associated with shear mode tests, as in the case of the compression shear block method ASTM D905-98 (1999a). Given some minimum quality of bonding, a high degree of wood failure is ensured because wood is weak in shear parallel to grain. This low shear strength, coupled with typical wood variables (i.e. minor grain deviations or growth-related density variation), creates significant scatter in the test results. Unfortunately, R&D personnel who are less familiar with wood are often frustrated by the seemingly indiscernible wood variations that hinder their efforts to achieve statistical power. In light of these frustrations, we wish to reintroduce the fracture approach as a useful alternative to wood adhesive testing; this is a complement to shear mode tests, not a replacement.

Consider a simple double cantilever beam, DCB, which is symmetrical about the adhesive layer, as in Fig. 1. Using linear elastic fracture mechanics, an energy balance is described when the DCB is loaded in opening, or mode I cleavage. Displacement energy input from the test frame is balanced against the sum of

† Member of SWST

Wood and Fiber Science, 33(3), 2001, pp. 377–385

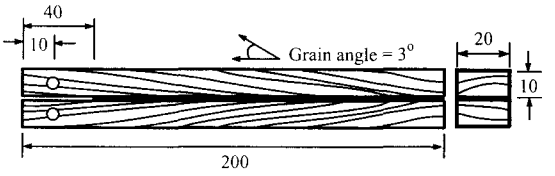

FIG. 1. Geometry and dimensions (in mm) of the flat DCB specimen used in this study.

two energies: potential energy stored in the DCB and that energy which is required to extend an interlaminar crack. The crack extension energy is often referred to as the mode I fracture energy, G_I, as follows (Kinloch 1987; Blackman et al. 1991):

$$G_I = \frac{P_c^2}{2B}\frac{dC}{da} \quad (1)$$

where P_c is the critical load when crack extension is initiated or arrested; B is the width of the DCB, and dC/da is the change in compliance, C, with the change in crack length, a.

This approach is by no means novel for the evaluation of wood adhesion. In fact, Ebewele, Koutsky, River and colleagues are credited for an impressive collection of works that demonstrate the great utility of mode I fracture testing for bonded wood. For example, the contoured DCB was used to evaluate several effects in wood bonding such as: wood grain angle (Ebewele et al. 1979; Mijovic and Koutsky 1979), resin cure time (Ebewele et al. 1979), wood surface roughness, surface aging (Ebewele et al. 1980), resin constitution (Ebewele et al. 1982, 1986a), and wood processing (Ebewele et al. 1986b). These works confirm that fracture testing is sensitive to intrinsic adhesive and adhesive bondline properties. Careful specimen preparation prevents wood failure. Therefore bulk wood properties and variability are factored out of the analysis. However, these early methods suffered from labor-intensive sample preparation. Solid wood contoured beams require special efforts for machining and bondline consolidation. This difficulty was alleviated with the development of composite specimens made from contoured aluminum beams and a flat adhesively laminated wood DCB (Scott et al. 1992; River et al. 1989). The flat wood DCB is consolidated in a standard press and later bonded to the contoured aluminum beams for analysis. Further improvements resulted when River and Okkonen replaced the aluminum with a constant tapered beam made from oriented strandboard, OSB (River and Okkonen 1993). Davalos et al. (1997) subsequently validated the constant taper, which is conveniently used for the composite contoured DCB; instead of OSB, laminated strand lumber was used. Use of the composite contoured DCB is still laborious and demanding with respect to calibration, wood selection, and sample preparation. For example, each reusable set of contoured beams may have a unique dC/da that must be determined through calibration of a composite specimen. Subsequent tests require careful density screening of wood adherends so as to maintain the validity of the original calibration. As mentioned, this method is quite powerful. Nevertheless, it is probable that the associated rigors have prevented the widespread adoption of fracture testing for bonded wood.

A tremendous simplification is realized if the cleavage test is conducted on the simple flat wood DCB as shown in Fig. 1. Notice, however, that dC/da is not linear for the flat DCB. Consequently, crack length measurements are required during testing. This is often perceived as a disadvantage for the flat specimen, whereas crack length measurements are unnecessary for contoured DCB specimens that have a linear dC/da (which must be determined with prior calibration). However, the turning point in favor of the flat DCB test has been realized with the development of computer automation and related digital hardware. This work demonstrates the benefits of the flat DCB, along with an established method of data analysis based upon beam theory.

MATERIALS AND METHODS

The lumber used was 51-mm-thick flat sawn yellow-poplar (*Liriodendron tulipifera*)

sapwood, knot-free. The adhesive was a phenol-formaldehyde impregnated paper film from DynoOverlays, 0.1-mm thickness.

Wood machining

Lumber is initially rough cut to rectangular shapes having a width (tangential face) of 200–250 mm and a length (longitudinal axis) of 240–250 mm. The 51-mm-wide radial faces are edged on a jointer to reveal the radial grain pattern. A three-degree grain angle is desired between the radial grain pattern and the longitudinal axis of the lumber (see Fig. 1). Lengthwise parallel lines are marked on the radial face to assist with bandsaw slicing. These lines are adjusted to compensate for any pre-existing slope of grain. The lumber is sliced on a bandsaw through the radial face into 15–17-mm-thick laminae. A large powerful bandsaw with a 25-mm or wider blade is required to maintain a straight slice. The laminae are then planed to a thickness of 11 mm, and placed into an environmental chamber. The samples in this study were conditioned at 20°C (±1°C) and 65% (±1%) relative humidity until they attained a 10% EMC, requiring approximately two weeks.

Laminate preparation

Immediately prior to adhesive application, bonding surfaces were planed to provide a final 10-mm thickness. Two laminae were paired so that the radial grain converged to a "V" shape at the bondline. The laminate assemblies, adhesive film sandwiched between two laminae, were placed between steel caul plates and then hot-pressed. With the press temperature set to 175°C (±5°C) and pressure fixed at 140 psi, five laminate assemblies were pressed each for 8, 12, 16, 20, or 24 min. A micromet IDEX® sensor and thermocouple were placed in the bondline of each assembly to enable microdielectric analysis of cure (Micromet Eumetrics®III dielectric analyzer; frequencies: 1, 10, 100, 1K, 100K Hz). After pressing and cooling, 10-mm-wide strips were removed from the laminate edges and discarded; specimens were ripped to final dimensions (Fig. 1). Each bonded laminate produced 3-4 fracture specimens. All specimens were then re-equilibrated in the environmental chamber, as above, to constant mass (±0.1 g). A precrack (30–40 mm) was initiated in the "open V" end of the specimens with a small bandsaw equipped with a fine blade. A preferred method involves the prevention of bonding in this precrack zone with the use of any number of release agents; a paraffin marker (crayon®) is very effective. Holes (4.4-mm diameter) were drilled into specimens for attachment to the test grips.

Test procedure

The procedure was adapted from ASTM D3433-93 (1999b). Mode I cleavage testing was performed on a screw-driven MTS Systems, Syntech 10/GL in displacement control mode. Data acquisition and system control were performed with TestWorks™ software. Crack lengths were monitored during testing using a CCD camera with 10 × magnification; a connected video monitor provided real-time crack measurements. The camera was mounted on a movable track, which allows one to center the moving crack tip in the field of view. A paper ruler with millimeter divisions was bonded below the bondline, and crack measurements were referenced from the point of loading. White typographic correction fluid was painted onto the bondline, providing a brittle high-contrast coating that simplifies crack visualization. Prior to loading, the free end of the fracture specimen was supported to maintain horizontal placement. Prior to data acquisition, a 5–10 Newton load was applied to the sample, and the crosshead position was zeroed. Loading was initiated at 1-mm/min displacement. When the computer detected a 3% drop in the load, resulting from crack extension, the crosshead was automatically held fixed for 45 s. This allowed the crack to extend and the load to become quasi-stable, where the change in load was less than 1 Newton. After the 45-s-hold time, the crosshead

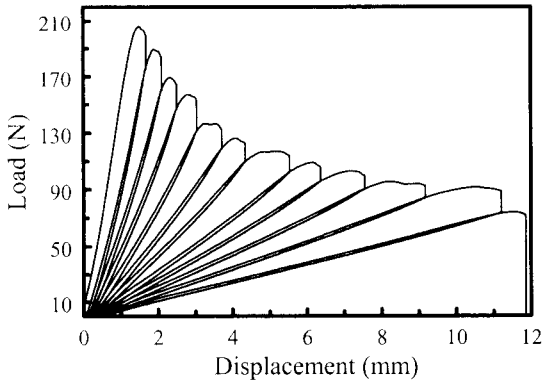

FIG. 2. A typical load-displacement curve obtained from a yellow-poplar DCB bonded with phenol-formaldehyde film adhesive.

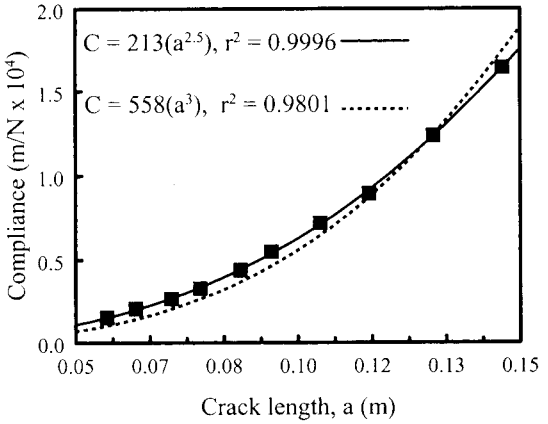

FIG. 3. A typical compliance versus crack length plot that is used for the direct compliance method of fracture energy calculation. Two fitted curves are shown, one for the cubic relationship and one for a simple power law as indicated.

was returned to zero displacement. This process was cycled until the sample failed catastrophically. The ASTM standard requires incremental increases in the displacement rate for each subsequent loading cycle so that fracture occurs on the order of 1 min. This ensures that the crack tip strain rate remains constant as the DCB lever arms extend with crack growth. The discreet displacement rates were calculated by dividing the opening displacement (in mm), from the arrest portion of the previous cycle, by 1 min. The data acquisition system recorded the maximum load, which typically occurs at crack initiation or briefly after initiation, and the load at crack arrest (the so called quasi-stable load mentioned above); displacement was measured using the MTS optical encoder, which is mounted directly to the crosshead ballscrew. The operator manually recorded the crack lengths at initiation and arrest. Care must be taken to ensure that the initiation and arrest loads are correctly assigned to the corresponding initiation and arrest crack lengths. Data points below 50 mm and above 150 mm of crack length were discarded.

Data analysis

Data analysis was conducted with two methods that are based on linear elastic fracture mechanics: 1) the direct compliance method, and 2) the shear corrected compliance method (Blackman et al. 1991).

Direct compliance method.—For each fracture specimen, the compliance is plotted against the corresponding crack length. Compliance is the reciprocal slope of each loading curve, (Fig. 2). A curve is fitted to the compliance versus crack length plot (Fig. 3). The equation of the best fit curve is differentiated with respect to "a" and then solved for each discreet initiation and arrest crack length. G_I is simply calculated from Eq. 1 for each initiation and arrest load with the corresponding dC/da. The curve fit was based upon the cubic relationship between compliance and crack length, as derived from beam theory (Blackman et al. 1991):

$$C = \frac{\delta}{P} = \frac{2a^3}{3EI} = ka^3 \qquad (2)$$

where δ is the displacement resulting from load P; E is the flexural modulus of the DCB arms, and I is the cross-sectional moment of inertia of one of these arms. In this analysis, we simply fit the final form of the equation, $C = ka^3$, where k is the fitted constant. As a comparison to the cubic relationship, a simple best fit power law was also applied.

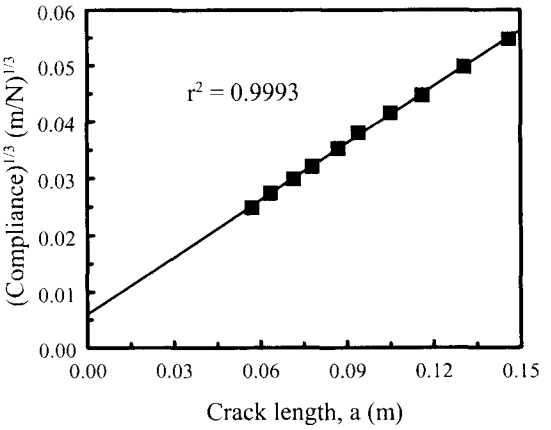

FIG. 4. A typical plot of the cube root of compliance versus crack length, using the data from Fig. 3.

Shear corrected compliance method.—Hashemi et al. (1990) have developed a modification of Eq. 1 that corrects for the low shear modulus of fiber-reinforced polymeric composites, as follows (Blackman et al. 1991):

$$G_I = \frac{P_c^2(a + x)^2}{B(EI)_{eff}} \tag{3}$$

where $(EI)_{eff}$ is the effective flexural rigidity of the DCB specimen, and x is the shear correction factor, or the crack length offset. These two parameters are determined from the experimental data by the following relationships:

$$(EI)_{eff} = \frac{2}{3m^3}; \tag{4a}$$

$$x = \frac{b}{m} \tag{4b}$$

where m and b are the slope and the y-intercept, respectively, from the linear trendline of the plot of the cube root of compliance versus crack length (Fig. 4). An example of this method of data analysis for epoxy/steel bonded systems is found in the literature (Rakestraw et al. 1995)

RESULTS AND DISCUSSION

For the following discussion, the term "laminate" refers to bonded samples with dimensions of approximately 200 × 250 mm; laminates are ripped into 3–4 individual fracture specimens.

A typical load/displacement plot is shown in Fig. 2. Minor hysteresis is seen in the noncoincidence of the loading and unloading curves. Furthermore, a slight displacement offset occurs on each loading cycle, totaling to about 0.5 mm of permanent set. The nature of this set was not noticeable to the eye; shapes of the fractured specimens were unchanged, and there was no apparent compression in the pin holes where loading occurred. These deviations from perfect elasticity appeared to be minor. An inelastic analysis could be applied (Kinloch and Tod 1984), but the improved accuracy may not outweigh the simplicity and convenience of the linear elastic treatment.

Two methods of data analysis were investigated, a direct compliance method and a shear corrected compliance method, as described above. A typical compliance versus crack length plot with fitted curves is shown in Fig. 3. Recall that the direct compliance method involves differentiation of the curve fit equations with respect to "a", providing dC/da and thus G_I via Eq. 1. It is apparent that the fit of the simple power law equation is superior to that for the cubic relationship. The cubic relationship ($C = ka^3$) is born from beam theory, while the power law was used simply for its improved fit. Fracture energies resulting from these curves are shown in Fig. 5 (for clarity's sake, only initiation/maximum energies are shown). Results from the power law fit are roughly independent of crack length, while results from the cubic relationship are not. One would expect G_I versus "a" to be flat (linear with slope = 0). In other words, G_I should be a material property of the system, allowing of course for wood surface variations along the bondline.

The shear corrected compliance method computes a crack length offset. This factor corrects for shear effects in adherends having a low shear modulus, in this case wood. It is obtained from the plot of the cube root of

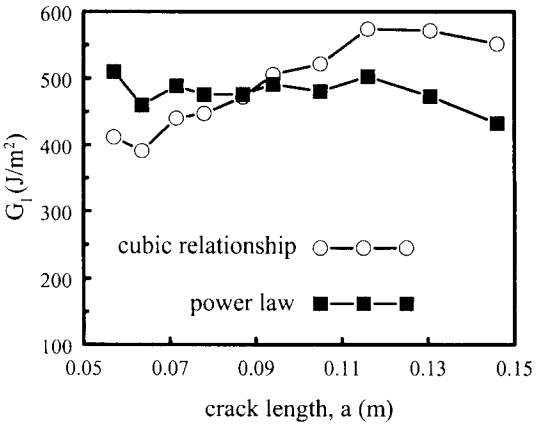

FIG. 5. A typical fracture energy versus crack length plot for a single fracture specimen. Results were calculated with the data of Fig. 3 using the direct compliance method based upon the cubic and simple power law curve fits as indicated.

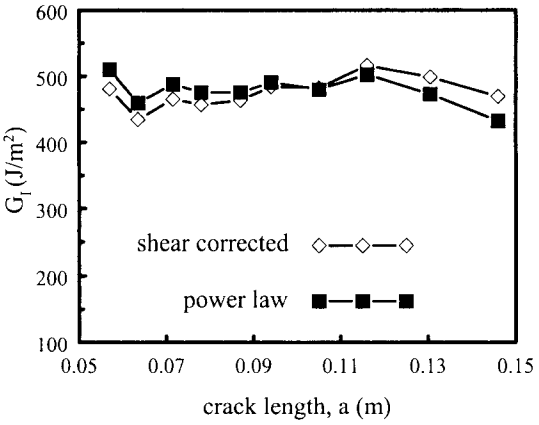

FIG. 6. Comparison of fracture energies calculated with the shear corrected compliance method and with the direct compliance method (using the simple power law fit) as indicated.

compliance versus crack length, as shown in Fig. 4. The excellent linearity shown in Fig. 4 is typical. The resulting fracture energies are in good agreement with those from the direct compliance method using the power law curve fit, (Fig. 6).

The preceding data analyses were conducted with a single data set from a representative fracture specimen. A more diagnostic comparison is found when evaluating the variability of the G_I versus crack length relationship within laminates (within cure time groupings). A single fracture specimen will produce about 10 G_I measurements, which means that a coefficient of variation, COV, of G_I could be calculated for each fracture specimen. Since 3–4 specimens are derived from one laminate, the average COV could be calculated for each laminate. Figure 7 shows the average COV(%) for two separate laminates, and it demonstrates that the variation in G_I is lowest when using the shear corrected compliance method. Again, a lower COV is expected because G_I should be independent of crack length. Therefore Fig. 7 indicates that the shear corrected compliance method provides the most reliable calculation of fracture energy. This method was used to investigate the effects of cure time of yellow-poplar bonded with a phenol-formaldehyde film adhesive.

Microdielectric analysis was used to monitor the cure of the yellow-poplar laminates; a typical conductivity plot is shown in Fig. 8. The onset of adhesive flow occurs at about 2 min as seen by the increase in conductivity; rapid crosslinking begins at about 7 min, and full cure appears to occur at 16–18 min. However, fracture tests indicate that significant changes in cure state occur between 16 and 24 min, as shown in Fig. 9 (In this figure, fracture energies were averaged within a specimen, and specimen means were averaged to give the laminate means for each hot-press time). The resistance to fracture is highest around 20 min, and it declines afterwards because of embrittlement from excessive crosslinking.

Figure 9 demonstrates that fracture testing is sensitive to intrinsic adhesive parameters. And as mentioned, careful grain angle control prevents wood failure. Consequently, post-fracture analysis is simplified because of the resulting smooth failure surfaces. Furthermore, this method provides a desirable level of statistical power. For example a single laminate supplies 3–4 fracture specimens, and each specimen produces 8–12 fracture energy measurements. This totals 24–48 data points

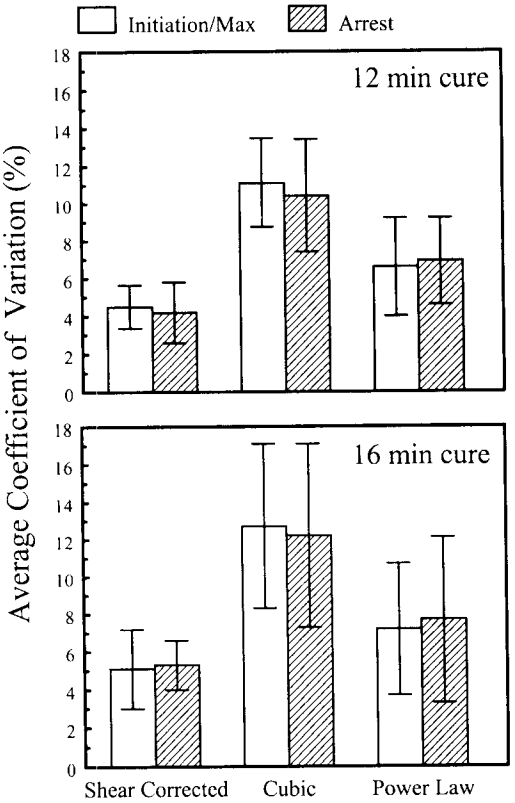

FIG. 7. Comparison of the average coefficient of variation in fracture energy as calculated with three different data analysis methods, for laminates cured for 12 and 16 minutes. The average COVs are derived from 4 fracture specimens for each cure time. Error bars indicate, plus or minus, one standard deviation.

that sample roughly 6000–8000 mm^2 of bondline, a relatively small area that provides an impressive amount of data (Note that various statistical groupings and treatments are possible; each has its theoretical merits and limitations). Interestingly, wood properties may vary considerably over this area, and this is conveniently monitored from the raw data. Recall that the flexural modulus is obtained from the slope of the $C^{1/3}$ versus crack length plot (Eq. 4a, b). Figure 10 shows the moduli so obtained for the specimens tested here. The average modulus was 12.1 GPa, which is in reasonable agreement with published values for yellow-poplar (Green et al. 1999). The COV (%) of moduli within bonded laminates

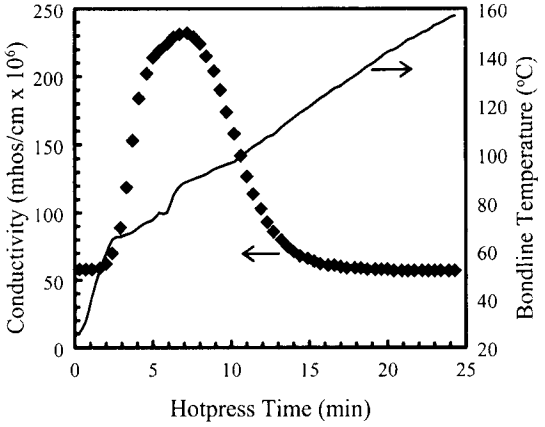

FIG. 8. Typical conductivity and bondline temperature data obtained from the microdielectric analysis of phenol-formaldehyde film adhesive curing in a yellow-poplar laminate.

ranges from 4.5% (hot-press time = 16 min) to 13.8% (hotpress time = 20 min). The modulus variation shown here is equal to or significantly greater than the corresponding variation in fracture energies. This is a very attractive and expected benefit of the method. The energy balance performed for each fracture specimen is based upon its unique mod-

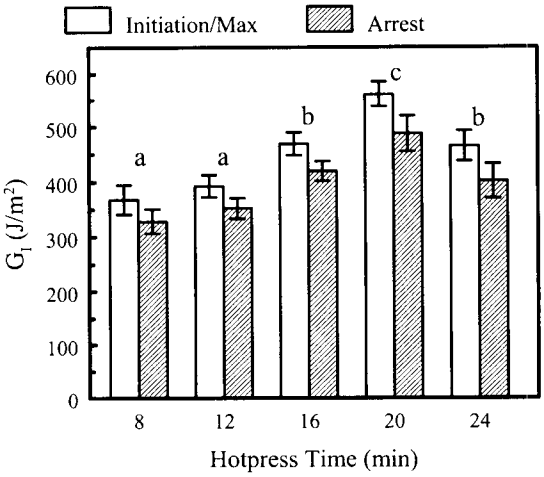

FIG. 9. Initiation/maximum and arrest fracture energies measured as a function of hot-press time. These laminate means are averages of the mean fracture energies within individual specimens. Error bars indicate, plus or minus, one standard deviation. Lowercase letters indicate statistically significant groupings.

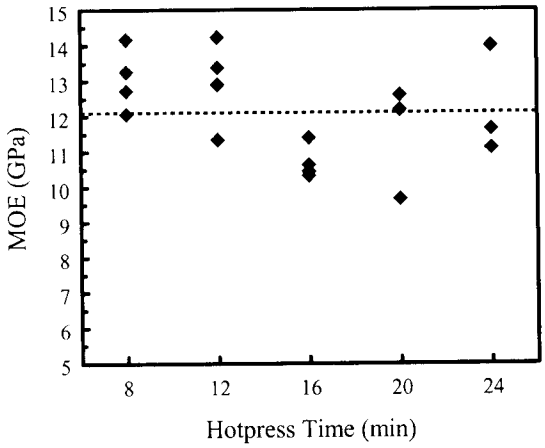

FIG. 10. Flexural moduli of all fracture specimens as obtained from the raw data via the shear corrected compliance method. The average modulus of all specimens is shown as the dotted line.

ulus as extracted from the raw data. Consequently, the variation in bulk wood modulus is factored out of this analysis. The resulting fracture energies arise from intrinsic adhesive and wood surface properties, where the latter exhibits the normal variability of course. An additional source of data variability may arise from the fact that individual fracture specimens cannot be perfectly symmetrical about the adhesive layer. This asymmetry must produce some mixture of mode I and mode II effects. This effect will be minor when the two bonded substrates have similar densities. However, a quantitative understanding of this issue would require numerical analysis.

This work affirms the great utility of fracture testing for adhesively-bonded wood, but this is nothing new. The value of fracture testing for bonded wood was clearly demonstrated over 20 years ago. However, the method has not been widely adopted because of the laborious sample preparation associated with the contoured DCB. The flat DCB eliminates much of this labor. Granted, machining for grain angle control is a complication relative to traditional shear mode tests. However, proficiency and productivity follow quickly after the technique is established. Likewise, a dedicated video system, and computer automation simplifies crack length measurements. Recent advances in digital hardware render flat DCB testing as an easier method. Others have previously employed the flat DCB (Lim et al. 1994; Lim and Mizumachi 1995); however, these studies did not benefit from the data analysis shown here. The shear corrected compliance method is powerful because of its ability to eliminate errors created by modulus variation. As mentioned, such modulus variation greatly confounds traditional shear mode tests.

Finally, those employing this method must cautiously apply the assumption of perfect linear elasticity. Plastic losses observed in this work were deemed minor. However, this assumption must be evaluated for each system. For example, inelastic behavior may be significant for thinner DCB specimens, for woods of very low specific gravity, or for adhesives with exceptional toughness. In such cases an inelastic analysis may be warranted.

CONCLUSIONS

Previous researchers have proven the outstanding value of the fracture approach for testing wood adhesion. These works employed the contoured double cantilever beam, a geometry that demands rigorous sample preparation, calibration, and wood selection. A tremendous simplification is realized with the flat double cantilever beam geometry. The flat geometry requires real-time crack length measurements, but current digital hardware reduces this to a routine task. An established data analysis method not previously applied to bonded wood proves to be simple, effective, and powerful. The improvements outlined above should enable more R&D personnel to adopt fracture methods for wood adhesive evaluation. This fracture method is still more demanding than traditional shear mode tests. Nevertheless, the simplifications shown here may provide sufficient incentive for others to benefit from the superior sensitivity of the fracture approach.

ACKNOWLEDGMENTS

For their helpful discussion and collaboration, special thanks go to Professor David Dil-

lard from the Engineering Science and Mechanics Department and to Professor Joseph Loferski from the Department of Wood Science and Forest Products, both at Virginia Tech.

REFERENCES

AMERICAN SOCIETY FOR TESTING AND MATERIALS. 1999a. Standard test method for strength properties of adhesive bonds in shear by compression loading. Annual Book of ASTM Standards. ASTM: D905-98, 15.06, 21–24.

AMERICAN SOCIETY FOR TESTING AND MATERIALS. 1999b. Standard test method for fracture strength in cleavage of adhesives in bonded metal joints. Annual Book of ASTM Standards. ASTM: D3433-93, 15.06, 212–224.

BLACKMAN, B., J. P. DEAR, A. J. KINLOCH, AND S. OSIYEMI. 1991. The calculation of adhesive fracture energies from double-cantilever beam test specimens. J. Mater. Sci. Lett. (10) 253–256.

DAVALOS, J. F., P. MADABHUSI-RAMAN, AND P. QIAO. 1997. Characterization of model-I fracture of hybrid material interface bonds by contoured DCB specimens. Eng. Fract. Mech. (58) 3:173–192.

EBEWELE, R., B. RIVER, AND J. KOUTSKY. 1979. Tapered double cantilever beam fracture tests of phenolic-wood adhesive joints. Part 1. Development of specimen geometry: Effects of bondline thickness, wood anisotropy, and cure time on fracture energy. Wood Fiber 11 (3): 197–213.

———, ———, AND ———. 1980. Tapered double cantilever beam fracture tests of phenolic-wood adhesive joints. Part II. Effects of surface roughness, the nature of surface roughness, and surface aging on joint fracture. Wood Fiber 12 (1):40–65.

———, ———, AND ———. 1982. Relationship between phenolic adhesive chemistry, cure and joint performance. Part I. Effects of base resin constitution and hardener on fracture energy and thermal effects during cure. J. Adhesion 14:189–217.

———, ———, AND ———. 1986a. Relationship between phenolic adhesive chemistry and adhesive joint performance; effect of filler type on fraction energy. J. Appl. Polym. Sci. (31):2275–2302.

———, ———, AND ———. 1986b. Wood processing variables and adhesive joint performance. J. Appl. Polym. Sci. (32):2979–2988.

GREEN, D. W., J. E. WINANDY, AND D. E. KRETSCHMANN. 1999. Mechanical properties of wood. Pagés 4:1–45 *in* Wood handbook, wood as an engineering material. Forest Products Society, Madison, WI.

HASHEMI, S., A. J. KINLOCH, AND J. G. WILLIAMS. 1990. The analysis of interlaminar fracture in uniaxial fibre-polymer composites. Proc. R. Soc. Lond. A (427):173–199.

KINLOCH, A. J. 1987. Adhesion and adhesives: Science and technology. Chapman & Hall, London, UK. 441 pp.

———, AND D. A. TOD. 1984. A new approach to crack growth in rubbery composite propellants. Propellants, Explosives, Pyrotech. (9):48–55.

LIM, W. W., AND H. MIZUMACHI. 1995. Fracture toughness of adhesive joints.II. Temperature and rate dependencies of mode I fracture toughness and adhesive strength. J. Appl. Polym. Sci. (57):55–61.

———, Y. HATANO, AND H. MIZUMACHI. 1994. Fracture toughness of adhesive joints. I. Relationship between strain energy release rates in three different fracture modes and adhesive strengths. J. Appl. Polym. Sci. (52): 967–973.

MIJOVIC, J. S., AND J. A. KOUTSKY. 1979. Effect of wood grain angle on fracture properties and fracture morphology of wood-epoxy joints. Wood Science 11 (3): 164–168.

RAKESTRAW, M. D. M. W. TAYLOR, D. A. DILLARD, AND T. CHANG. 1995. Time dependent crack growth and loading rate effects on interfacial and cohesive fracture of adhesive joints. J. Adhesion (55):123–149.

RIVER, B. H., AND E. A. OKKONEN. 1993. Contoured wood double cantilever beam specimen for adhesive joint fracture tests. J. Testing Eval. (21):1, 21–28.

———, C. T. SCOTT, AND J. A. KOUTSKY. 1989. Adhesive joint fracture behavior during setting and aging. Forest Prod. J. 39 (11/12):23–28.

SCOTT, C. T., B. H. RIVER, AND J. A. KOUTSKY. 1992. Fracture testing wood adhesives with composite cantilever beams. J. Testing Eval. 20 (4):259–264.